Reconciling plate kinematic and seismic estimates of lithospheric convergence in the central Indian Ocean

J.M. Bull[1], C. DeMets[2], K.S. Krishna[3], D.J. Sanderson[4], and S. Merkouriev[5]

[1]School of Ocean and Earth Science, National Oceanography Centre Southampton, University of Southampton, Southampton SO14 3ZH, UK

[2]Department of Geoscience, University of Wisconsin-Madison, Madison, Wisconsin 53706, USA

[3]National Institute of Oceanography, Council of Scientific and Industrial Research, Dona Paula, Goa 403004, India

[4]School of Civil Engineering and the Environment, University of Southampton, Southampton SO17 1BJ, UK

[5]St. Petersburg Filial of Institute of Terrestrial Magnetism, Ionosphere and Radio Wave Propagation (SPbFIZMIRAN), Muchnoj per, 2, Box 188, St. Petersburg, Russia

ABSTRACT

The far-field signature of the India-Asia collision and history of uplift in Tibet are recorded by sediment input into the Indian Ocean and the strain accumulation history across the diffuse plate boundary between the Indian and Capricorn plates. We describe the history of India-Capricorn convergence from updated estimates of India-Somalia-Capricorn plate rotations and observations derived from seismic reflection data. New India-Capricorn plate rotations for the past 20 m.y. are consistent with slow north-south convergence from 18 Ma about a stationary or nearly stationary pole near the eastern edge of the Chagos-Laccadive ridge, simpler than predicted by previous models based on many fewer data. The new rotations suggest that convergence began between 18 and 14 Ma, consistent with marine seismic evidence for an onset of deformation at 15.4–13.9 Ma. They further show that convergence rates doubled at 8 Ma, in agreement with a sharp increase in fault activity at 8–7.5 Ma seen on seismic reflection profiles. A discrepancy between the total strain estimated from kinematic and seismic reflection data can be reconciled if pervasive reverse faulting within the diffuse plate boundary is accompanied by block rotations of 1°–3°.

INTRODUCTION

The deformation zone within the central Indian Ocean is the best-studied diffuse plate boundary zone in the oceans (Fig. 1). The deformation is manifest on two spatial scales: reverse faulted blocks with 5–10 km spacing, and 100–300-km-wavelength folding of the oceanic lithosphere. The deformation has been described by seismic reflection, heat flow, studies of intraplate seismicity, and satellite gravity studies (e.g., Weissel et al., 1980; Bull and Scrutton, 1990a; Chamot-Rooke et al., 1993; Deplus et al., 1998; Delescluse et al., 2008; Delescluse and Chamot-Rooke, 2007). Motion across the diffuse plate boundary zone has been estimated independently from inversions of seafloor spreading rates and directions from the Carlsberg and Central Indian ridges and consists of counterclockwise rotation about a pole east of Chagos Bank (Royer and Gordon, 1997; Gordon et al., 1998; DeMets et al., 2005), such that convergence is predicted in the Central Indian and Wharton Basins, and extension west of Chagos Bank.

Seismic stratigraphic analysis of the Bengal Fan sediments has revealed that the main deformation phase began in the Miocene (8.0–7.5 Ma; Cochran, 1990) and included long-wavelength folding, development of a regional unconformity, pervasive reverse faulting, with continuation of long-wavelength folding and faulting in the Pliocene (5.0–4.0 Ma) and Pleistocene (0.8 Ma) (Krishna et al., 2001). Plate reconstructions independently confirm the onset of rapid deformation at 8–7 Ma (DeMets et al., 2005), and moreover suggest that significant, but slower deformation began as early as 20 Ma with large uncertainties. Seismic stratigraphic data (Krishna et al., 2009) suggest that slow deformation began at 15.4–13.9 Ma.
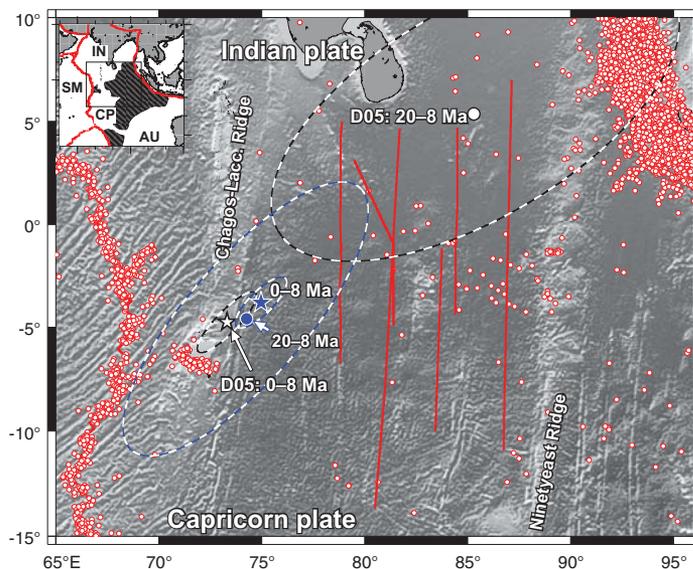
Figure 1. Location map of study area. Red circles show shallow earthquakes from 1963 to 2008, all magnitudes, from U.S. National Earthquake Information Center database. Red lines show locations of seismic profiles described in text. Solid blue star and circle show 8–0 Ma and 20–8 Ma Capricorn-India pole locations for this study, respectively. White star and circle labeled D05 show Capricorn-India 8–0 Ma and 20–8 Ma poles from DeMets et al. (2005). Ellipses show two-dimensional, 1σ uncertainties. Inset shows extent of major plates and diffuse plate boundaries (stripes); CP—Capricorn; IN—India; SM—Somalia; AU—Australia.

Although previous independent analyses of seismic stratigraphic and plate kinematic data from the central Indian Ocean confirm important aspects of the style and timing of deformation across the wide plate boundary south of India, important discrepancies and uncertainties remain. For example, the most recent model for India-Capricorn plate motion (DeMets et al. 2005) predicts a systematic increase in the magnitude of north-south shortening across the India-Capricorn boundary zone east of the pole of rotation, whereas a recent analysis of seismic reflection data suggests a more complex pattern (Krishna et al., 2009). Cumulative north-south strain smaller than predicted from plate rotations has been found (Krishna et al., 2009), suggesting that unaccounted errors exist in one or both estimates, or that some deformation occurs either outside the diffuse boundary or via mechanisms not considered in these studies.

Here we derive new India-Capricorn finite rotations for the past 20 m.y. from recently published, high-resolution India-Somalia and Capricorn-Somalia rotations. We then compare these predictions with new

shortening estimates from seismic reflection data that are based on rotations of reversely faulted blocks.

UPDATED PLATE KINEMATIC ESTIMATE

The new India-Capricorn-Somalia rotations (Tables DR1–DR3 in the GSA Data Repository[1]) are derived from new high-resolution estimates of India-Somalia motion since 20 Ma (Merkouriev and DeMets, 2006) and Capricorn-Somalia finite rotations (from DeMets et al., 2005). The India-Somalia rotations are determined from an order-of-magnitude more magnetic anomaly crossings than those of DeMets et al. (2005) and describe a simpler and better constrained post–20 Ma kinematic history than prior models. We corrected both sets of rotations for the effect of outward displacement, which shifts the midpoints of magnetic reversals several kilometers outward from spreading axes due to the finite width of the zone in which new seafloor acquires its magnetization (DeMets and Wilson, 2008). Information about the methods used to estimate the new rotations is given in the Data Repository.

Interval spreading rates determined from the updated Capricorn-Somalia and India-Somalia rotations (Fig. DR1) illustrate the primary kinematic evidence for a change in India and Capricorn plate motions at 8–10 Ma, as discussed by Merkouriev and DeMets (2006). Spreading rates along both boundaries decreased by 25%–30% from 20 Ma to ca. 10 Ma, and then remained steady or increased slightly to the present. The newly estimated interval rates are less noisy than their predecessors (Merkouriev and DeMets, 2006) and clearly suggest two distinct stages of motion for both plate pairs since 20 Ma.

The new best-fitting India-Capricorn poles (Fig. 2; Table DR3) are all located within several hundred kilometers of the eastern edge of the Chagos-Laccadive ridge and show no dependence on age. For example, the rotations that describe motion from the present to 8 Ma and from 8 to 20 Ma (Fig. 1) differ insignificantly in location and predict that approximate north-south shortening dominated deformation nearly everywhere along the plate boundary during their respective time intervals. In contrast, the 20–8 Ma pole determined from rotations in DeMets et al. (2005) is 1200 km northeast of the 8–0 Ma estimate (Fig. 1) and predicts a component of extension across more than two-thirds of the India-Capricorn boundary before 8 Ma, in conflict with evidence for shortening at that time (Krishna et al., 2009). The new India-Capricorn rotation estimates therefore yield a simpler kinematic history that agrees better with the independently determined shortening history across the diffuse plate boundary than was previously the case.

We interpret the new results as evidence that India-Capricorn motion since 20 Ma is well described by a stationary pole (at 3.7°S, 74.8°E in Fig. 1) located at the Fisher mean of the best-fitting rotations. That the stationary pole is near the eastern edge of the Chagos-Laccadive ridge, which consists of unusually thick oceanic crust formed by the Reunion mantle plume (Henstock and Thompson, 2004), may indicate that the ridge plays a mechanical role in determining the pole location.

Using the stationary India-Capricorn pole described above, we apply procedures described by DeMets et al. (2005) to estimate an optimized time sequence of rotation angles (upper panel of Fig. 2). The new sequence of angles can be interpreted as evidence for either a two-stage or three-stage rotation history. Both include the previously reported factor of two increase in India-Capricorn motion since 8 Ma (DeMets and Royer, 2003; DeMets et al., 2005), and the three-stage rotation history subdivides motion before 8 Ma into periods of slow or possibly no motion before ca. 16 ± 2 Ma and somewhat faster motion from ca. 16 ± 2 Ma to 8 Ma.
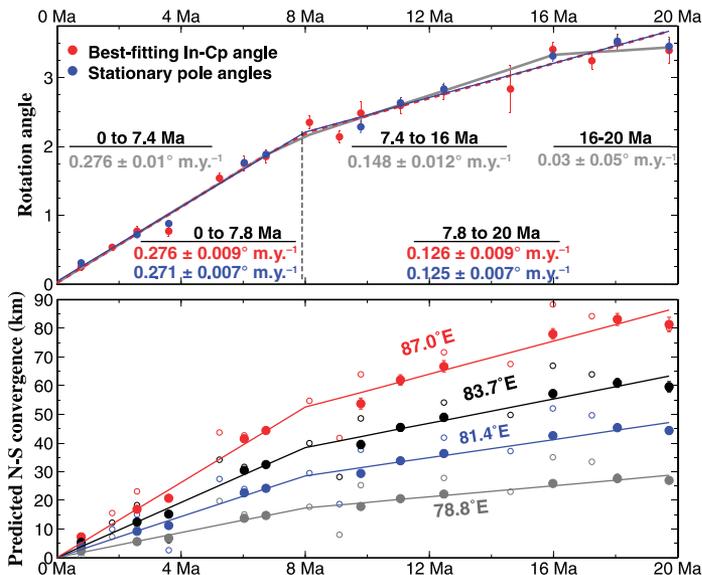
Figure 2. Upper: India-Capricorn (In-Cp) finite rotation angles and standard errors for best-fitting poles from Table DR4 (see footnote 1) and for 0–20 Ma stationary pole at 3.74°S, 74.76°E. Stationary pole angles are procedurally limited to magnetic reversals for which identical crossing points were used to reconstruct Capricorn-Somalia (DeMets et al. 2005) and India-Somalia (Merkouriev and DeMets, 2006) plate positions. Gray lines indicate best-fitting three-stage rotation history described in text. Red and blue lines show best-fitting, least-squares two-stage history for both sets of rotation angles. Ages for changes in motion were estimated as part of inversion procedure and give a best age of 7.8 ± 1 Ma. Lower: Predicted north-south shortening component across India-Capricorn plate boundary, 0–20 Ma. Shortening is predicted at 3.5°S at longitudes of four seismic profiles shown in Figure 1. Filled and open symbols are derived from stationary-pole and best-fitting India-Capricorn rotations, respectively.

Inversions of the angles in Figure 2 to estimate best-fitting slopes and ages for changes in motion for the two- and three-stage models indicate that a motion change at 7.8 Ma is highly significant, but that any earlier change cannot be distinguished reliably from the sparse and less certain angles for times before 13 Ma.

SEISMIC REFLECTION ANALYSIS

In the most recent synthesis of seismic reflection data (Krishna et al., 2009), measurements were made on the vertical separations of sedimentary horizons and unconformities on either side of 293 reverse faults. These data were then backstripped to determine fault activity histories. These data indicate that near or prior to 20 Ma, isolated faults accommodated minor extensional movement before a period of tectonic quiescence. Compressional activity then began on individual fault blocks at 15.4–13.9 Ma and continued to 8.0–7.5 Ma. Strain rates increased abruptly at 8.0–7.5 Ma, which led to widespread reverse faulting and the formation of long-wavelength undulations and the first regional unconformity, and have continued to present.

Previously, workers calculated the cumulative shortening accommodated by reverse faulting across the diffuse plate boundary (Chamot-Rooke et al., 1993; Van Orman et al., 1995; Krishna et al., 2009) using a three-stage procedure. Vertical separations of sedimentary reflectors immediately above basement are first measured and depth converted using the velocity law in Bull and Scrutton (1990b). These were assumed to approximate fault throws, and the horizontal (shortening) component was calculated using dips (36°–45°) for the reverse faults in the top of the

oceanic crust estimated from the seismic reflection data (e.g., Bull and Scrutton, 1992; Chamot-Rooke et al., 1993). This approach has yielded total strain estimates of 1.9%–4.3% across the diffuse boundary. Long-wavelength undulations in the central Indian Ocean accommodate <1% of the total shortening across the diffuse plate boundary and are thus ignored in the following.

The procedure outlined above has three limitations that are likely to produce underestimates of the shortening: (1) the vertical separations are made in poorly imaged regions above and below the fault surface and incorporate drag; (2) the vertical separation is less than the throw for dipping horizons; and (3) the method ignores the likely contribution of fault block rotation to the estimated shortening. In the Central Indian Basin, seismic reflection data from faulted blocks (Fig. 3) clearly show that the top of layer 2 is rotated by 1°–3° relative to horizontal (Fig. 3A), with some fault blocks rotated by 6°–8° (Fig. 3B). Previously published shortening estimates may thus underestimate the total shortening across the diffuse plate boundary.

We therefore recalculated shortening due to reverse faulting by applying a method widely used for rotational extensional faults, the "domino" model of Wernicke and Burchfiel (1982). This provides an independent estimate of shortening without the problems inherent in determining heave from cutoffs at faults, and incorporates the observed rotations. The method requires an estimate of the dip of each reverse fault and the rotation of each fault block (Fig. 3C), which can be approximated by the dip of the top of the oceanic crust. Reliable measurements of the latter are only

feasible with multichannel seismic reflection data, which consistently image the top of basement (Bull and Scrutton, 1992; Chamot-Rooke et al., 1993). Multichannel data coverage is, however, much sparser than the single-channel data synthesized by Van Orman et al. (1995) and Krishna et al. (2009), thereby precluding an observationally based correction for each fault that has been imaged in the diffuse plate boundary. We therefore reestimated the total shortening for a range of plausible fault block rotations ($\omega = 1°–3°$), an average fault dip (δ) of 40°, and using profile lengths at each longitude defined by the distance between the most widely distributed faults (see Krishna et al., 2009). These give revised shortening estimates of 2.1% to 6.4%, which result in between 17 and 52 km of north-south convergence at 78.8°E, increasing eastward to between 34 and 104 km of convergence at 87°E (Fig. 4). The higher value exceeds previous maximum shortening estimates from seismic reflection data, most likely due to the problems described here in measuring vertical displacement across faults.
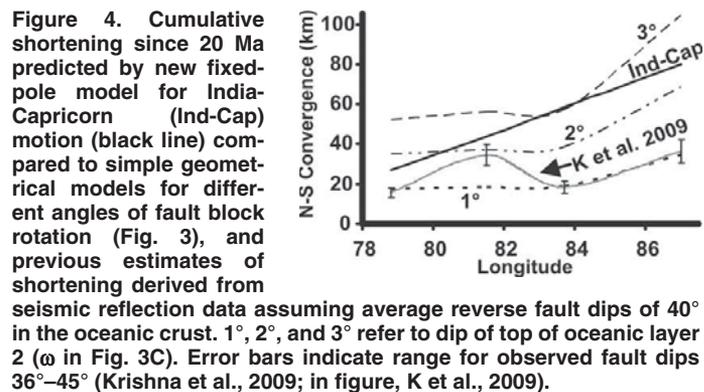
Figure 4. Cumulative shortening since 20 Ma predicted by new fixed-pole model for India-Capricorn (Ind-Cap) motion (black line) compared to simple geometrical models for different angles of fault block rotation (Fig. 3), and previous estimates of shortening derived from

seismic reflection data assuming average reverse fault dips of 40° in the oceanic crust. 1°, 2°, and 3° refer to dip of top of oceanic layer 2 (ω in Fig. 3C). Error bars indicate range for observed fault dips 36°–45° (Krishna et al., 2009; in figure, K et al., 2009).

Figure 3. Seismic reflection images of tilted fault blocks bounded by reverse faults and the simple geometrical construction used to calculate shortening. A: Fault block (representative of deformational area) with dip on top of layer 2 of 2°–3°. TWT—two-way traveltime. B: Fault blocks showing maximum amount of rotation with dip on top of layer 2 of 4°–8°. Calculations of fault dip use velocity law of Bull and Scrutton (1990b). C: Simple geometrical construction used to calculate shortening based solely on dip of reverse faults in upper part of oceanic crust (δ), and dip of top of oceanic crust layer 2 (ω) (see text for discussion). L—fault block width; L_0—original fault block width.

SYNTHESIS AND CONCLUSIONS

Here we summarize where our new plate kinematic analysis (Fig. 2) reconciles previous differences with seismic stratigraphic studies, and where differences remain. There is striking agreement concerning the acceleration of convergence and associated contractional deformation at 8 Ma, with a well-defined factor of two increase in the rate of angular rotation contemporaneous with the development of a regional unconformity related to the formation of long-wavelength (100–300 km) folds, and an increase in reverse faulting activity seen on the seismic reflection profiles (Krishna et al., 2009). Both methods agree that convergence (and associated contractional deformation) began earlier, and more slowly, than at 8 Ma. We show how a simple rotational model for reverse fault blocks can be used to reconcile the total amount of convergence across the diffuse plate boundary zone.

Additional work is needed to better resolve the history of India-Capricorn motion before 10 Ma. Whereas seismic stratigraphic–derived estimates indicate that convergence began at 15.4–13.9 Ma, the India-Capricorn rotation history allows for an onset of convergence as early as 18 Ma (Fig. 2). A conservative interpretation of these results is that slow convergence began between 18 and 13.9 Ma. Better stratigraphic age control from future Integrated Ocean Drilling Program (IODP) study sites in the Bengal Fan is needed to reduce the uncertainty in our stratigraphic estimate, which relies on extrapolation of rates from a single drill site (ODP Leg 116). Analyses of additional magnetic anomalies are needed to improve the limited temporal resolution and uncertainties for rotations for times before 13 Ma, as well as test whether the negative rotation angle from 20 to 18 Ma, coinciding with a period of possible normal faulting observed by Krishna et al. (2009), is supported by additional reconstructions. Our new kinematic estimates do not reveal possible discrete phases

of deformation at 5.0–4.0 Ma and 0.8 Ma inferred from seismic reflection data (Krishna et al. 2001), and are instead most simply interpreted as consistent with steady motion about a fixed pole since ca. 8 Ma (Fig. 2).

The cumulative shortening estimate of Krishna et al. (2009) from seismic reflection data (Fig. 4) is smaller than predicted by our updated and previous kinematic models for all four of the seismic profiles included in their analysis (Fig. 4), with differences of ~40 km for two profiles that greatly exceed the estimated uncertainties (±10 km). Given that all four profiles span almost all of the most intensely deforming areas of the plate boundary (Fig. 1), it seems unlikely that the discrepancy between the two independent shortening estimates can be attributed to structures not imaged by the seismic profiles. Similarly, the plate kinematic estimates are based on numerous unambiguous magnetic and bathymetric data, and are both robust and have well-characterized uncertainties.

We demonstrate here that previous shortening estimates from seismic reflection data were too low. Our new estimates of total shortening for assumed average fault block rotations of 2°–3° and average fault dips of 40° (Fig. 4) bracket the shortening estimates predicted by our updated kinematic model, and thus fully reconcile the two independent estimates. Although not all the fault blocks show evidence for rotation, and some fault blocks (e.g., Fig. 3B) are rotated more than 3°, we find it encouraging that such a simple geometric model can resolve the previously large discrepancy between the shortening estimates.

Reasons for the onset of convergence at 18–14 Ma are unclear, as are the causes of the sharp increase in deformation at 8 Ma: we know of no significant changes in spreading rates or directions at the Indian Ocean ridge system at these times. We follow others (e.g., Molnar and Stock, 2009; Gordon, 2009) in suggesting that the answers must lie within the history of Tibet, the uplift of which caused increased deviatoric stresses over a wide area, including the equatorial Indian Ocean. We note that a recent analysis of motion between the Indian and Eurasian plates (Molnar and Stock, 2009), although having less temporal resolution than our study, is consistent with an event at 17 Ma causing a slowing of India-Eurasia convergence. That the India-Capricorn rotation pole since ca. 18 Ma has remained stationary and adjacent to the Chagos-Laccadive ridge may indicate that the ridge played a mechanical role in determining the pole location and hence deformation across the wide equatorial plate boundary.

REFERENCES CITED
Bull, J.M., and Scrutton, R.A., 1990a, Fault reactivation in the central Indian Ocean and the rheology of oceanic lithosphere: Nature, v. 344, p. 855–858, doi: 10.1038/344855a0.
Bull, J.M., and Scrutton, R.A., 1990b, Sediment velocities and deep structure from wide-angle reflection data around Leg 116 sites, in Cochran, J.R., et al., Proceedings Ocean Drilling Program, Scientific results, Volume 116: College Station, Texas, Ocean Drilling Program, p. 311–316.
Bull, J.M., and Scrutton, R.A., 1992, Seismic reflection images of intraplate deformation, central Indian Ocean, and their tectonic significance: Geological Society of London Journal, v. 149, p. 955–966, doi: 10.1144/gsjgs.149.6.0955.
Chamot-Rooke, N., Jestin, F., de Voogd, B., and Phedre Working Group, 1993, Intraplate shortening in the central Indian Ocean determined from a 2100-km-long north-south deep seismic reflection profile: Geology, v. 21, p. 1043–1046, doi: 10.1130/0091-7613(1993)021<1043:ISITCI>2.3.CO;2.
Cochran, J.R., 1990, Himalayan uplift, sea level, and the record of Bengal Fan sedimentation at the ODP Leg 116 sites, in Cochran, J.R., et al., Proceedings of the Ocean Drilling Program, Scientific results, Volume 116: College Station, Texas, Ocean Drilling Program, p. 397–414.
Delescluse, M., and Chamot-Rooke, N., 2007, Instantaneous deformation and kinematics of the India-Australia plate: Geophysical Journal International, v. 168, p. 818–842, doi: 10.1111/j.1365-246X.2006.03181.x.
Delescluse, M., Montési, L.G.J., and Chamot-Rooke, N., 2008, Fault reactivation and selective abandonment in the oceanic lithosphere: Geophysical Research Letters, v. 35, L16312, doi: 10.1029/2008GL035066.
DeMets, C., and Royer, J.-Y., 2003, A new high-resolution model for India-Capricorn motion since 20 Ma: Implications for the chronology and magnitude of distributed crustal deformation in the Central Indian Basin: Current Science, v. 85, p. 339–345.
DeMets, C., and Wilson, D.S., 2008, Toward a minimum change model for recent plate motions: Calibrating seafloor spreading rates for outward displacement: Geophysical Journal International, v. 174, p. 825–841, doi: 10.1111/j.1365-246X.2008.03836.x.
DeMets, C., Gordon, R.G., and Royer, J.-Y., 2005, Motion between the Indian, Capricorn and Somalian plates since 20 Ma: Implications for the timing and magnitude of distributed lithospheric deformation in the equatorial Indian Ocean: Geophysical Journal International, v. 161, p. 445–468, doi: 10.1111/j.1365-246X.2005.02598.x.
Deplus, C., Diament, M., Hebert, H., Bertrand, G., Dominguez, S., Dubois, J., Malod, J., Patriat, P., Pontoise, B., and Sibilla, J.J., 1998, Direct evidence of active deformation in the eastern Indian oceanic plate: Geology, v. 26, p. 131–134, doi: 10.1130/0091-7613(1998)026<0131:DEOADI>2.3.CO;2.
Gordon, R.G., 2009, Lithospheric deformation in the equatorial Indian Ocean: Timing and Tibet: Geology, v. 37, p. 287–288, doi: 10.1130/focus032009.1.
Gordon, R.G., DeMets, C., and Royer, J.-Y., 1998, Evidence for long-term diffuse deformation of the lithosphere of the equatorial Indian Ocean: Nature, v. 395, p. 370–374, doi: 10.1038/26463.
Henstock, T.J., and Thompson, P.J., 2004, Self-consistent modeling of crustal thickness at Chagos-Laccadive Ridge from bathymetry and gravity data: Earth and Planetary Science Letters, v. 224, p. 325–336, doi: 10.1016/j.epsl.2004.05.021.
Krishna, K.S., Bull, J.M., and Scrutton, R.A., 2001, Evidence for multiphase folding of the central Indian Ocean lithosphere: Geology, v. 29, p. 715–718, doi: 10.1130/0091-7613(2001)029<0715:EFMFOT>2.0.CO;2.
Krishna, K.S., Bull, J.M., and Scrutton, R.A., 2009, Early (pre-8 Ma) fault activity and temporal strain accumulation in the central Indian Ocean: Geology, v. 37, p. 227–230, doi: 10.1130/G25265A.1.
Merkouriev, S., and DeMets, C., 2006, Constraints on Indian plate motion since 20 Ma from dense Russian magnetic data: Implications for Indian plate dynamics: Geochemistry Geophysics Geosystems, v. 7, Q02002, doi: 10.1029/2005GC001079.
Molnar, P., and Stock, J.M., 2009, Slowing of India's convergence with Eurasia since 20 Ma and its implications for Tibetan mantle dynamics: Tectonics, v. 28, TC3001, doi: 10.1029/2008TC002271.
Royer, J.-Y., and Gordon, R.G., 1997, The motion and boundary between the Capricorn and Australian plates: Science, v. 277, p. 1268–1274, doi: 10.1126/science.277.5330.1268.
Van Orman, J., Cochran, J.R., Weissel, J.K., and Jestin, F., 1995, Distribution of shortening between the Indian and Australian plates in the central Indian Ocean: Earth and Planetary Science Letters, v. 133, p. 35–46, doi: 10.1016/0012-821X(95)00061-G.
Weissel, J.K., Anderson, R.N., and Geller, C.A., 1980, Deformation of the Indo-Australian plate: Nature, v. 287, p. 284–291, doi: 10.1038/287284a0.
Wernicke, B., and Burchfiel, B.C., 1982, Modes of extensional tectonics: Journal of Structural Geology, v. 4, p. 105–115, doi: 10.1016/0191-8141(82)90021-9.